

Photonic crystals with small metal inclusions

Alexander Moroz

Soft Condensed Matter, Debye Institute, Utrecht University, Utrecht, The Netherlands

ABSTRACT

It is shown that small metallic inclusions can have a dramatic effect on the photonic band structure of diamond and zinc blende structures. In the case of silica spheres with a silver core, the complete photonic band gap (CPBG) between the 2nd-3rd bands opens for a metal volume fraction $f_m \approx 1\%$ and has a width of 5% for $f_m \approx 2.5\%$. Absorption in the CPBG of 5% remains very small ($\leq 2.6\%$ for $\lambda \geq 750$ nm). These findings open the door for any semiconductor and polymer material to be used as a genuine photonic crystal building block and significantly increase the possibilities for experimentalists to realize a sizeable and robust CPBG in the near-infrared and in the visible.

Keywords: photonic crystals, nanostructured materials, colloids

1. INTRODUCTION

Photonic crystals are structures with a periodically modulated dielectric constant. In analogy to the case of an electron moving in a periodic potential, light propagating in a photonic crystal experiences multiple scattering leading to the formation of Bloch waves and photonic band gaps.¹⁻³ If the bandgap persists for both polarizations and all directions of propagation one speaks of a complete photonic bandgap (CPBG).^{4,5} Light with frequencies within a CPBG is totally reflected since it cannot propagate inside the crystal. Yet light can propagate through waveguides carefully designed within such a photonic crystal, even when such a waveguide has sharp bends.⁶ In the last decade, photonic crystals have enjoyed a lot of interest in connection with their possibilities to guide light and to become a platform for the fabrication of photonic integrated circuits.^{3,6} There is a common belief that, in the near future, photonic crystals systems will allow us to perform many functions with light that ordinary crystals do with electrons. In addition to numerous potential technological applications (filters, optical switches, superprisms, cavities, etc³), photonic crystals also promise to become a laboratory for testing fundamental processes involving interactions of radiation with matter under novel conditions.^{1,2} The presence of a CPBG causes dramatic changes in the local density of states, which offers the possibility to control and engineer the spontaneous emission of embedded atoms and molecules.¹

For applications one needs a sufficiently large CPBG to leave a margin for gap-edge distortions due to omnipresent defects.⁷ Let us define the relative gap width g_w as the gap width-to-midgap frequency ratio, $\Delta\omega/\omega_c$. Then in order to achieve g_w larger than 5%, the dielectric contrast ≥ 9.8 and ≥ 12 is required for a diamond⁸ and face-centered-cubic (fcc) structure,⁹ respectively. This leaves only a couple of materials for photonic crystals applications at near infrared and optical wavelengths.¹⁰ Surprisingly enough, it will be demonstrated here that there is a way to create a sizeable and robust CPBG in the near-infrared and in the visible even with silica glass or a polymer. The trick is to place small inclusions of a low absorbing metal in the right dielectric structure. It turns out that the effect of small inclusions of a low absorbing metal on the photonic bandgap structure is very strong for diamond and zinc-blende structures (see Fig. 1). The photonic properties of these structures, which are calculated using the multiple-scattering theory for electromagnetic waves (see Sec. 2), are reviewed in Sec. 3. Only the case of the close-packed case of spheres in air was investigated. This case can be soon fabricated either by “do-it-yourself organization”³ or by a microrobotic technique.³ At the same time, when starting from colloidal suspension, one expects to use dried structures in air for practical applications which will most probably consist of touching spheres (close-packed structures).

Further author information:

Address: Soft Condensed Matter, Debye Institute, Utrecht University, Postbus 80000, 3508 TA Utrecht, The Netherlands
http://www.amolf.nl/research/photonic_materials_theory/moroz/moroz.html

E-mail: moroz@phys.uu.nl

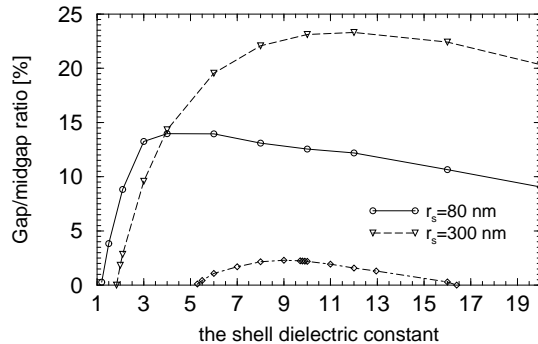


Figure 1. Gap width to midgap frequency ratio of the 2nd-3rd CPBG for a close-packed metallo-dielectric diamond lattice of silver core - dielectric shell spheres with a fixed ratio of the core and sphere radii $r_c/r_s = 0.5$ ($f_m = 4.25\%$) in air as a function of the shell dielectric constant for the cases $r_s = 80$ nm and $r_s = 300$ nm. For a comparison, the dot-dashed line with diamonds shows the gap to midgap frequency ratio of the 2nd-3rd CPBG of a close-packed diamond lattice of purely dielectric spheres.

2. MULTIPLE-SCATTERING THEORY FOR ELECTROMAGNETIC WAVES

Let Λ be a simple (Bravais) periodic lattice in three dimensions. According to the Bloch theorem, propagating wave ψ in a periodic structure with the symmetry Λ is characterized by the Bloch momentum \mathbf{k} . The latter describes translational properties of ψ by any lattice vector $\mathbf{r}_s \in \Lambda$,

$$\psi(\mathbf{r} + \mathbf{r}_s) = \psi(\mathbf{r}) \exp(i\mathbf{k} \cdot \mathbf{r}_s). \quad (1)$$

The Bloch property holds irrespective of the spin of a wave, i.e., is the same for scalar and vector waves. We shall confine ourselves to the case when, outside scatterers, wavefunction ψ satisfies the scalar Helmholtz equation,

$$[\Delta + \sigma^2]\psi = 0, \quad (2)$$

with σ being a positive constant. Let $G_{0\Lambda}(\sigma, \mathbf{k}, \mathbf{R})$ denote the free-space periodic Green's function of the Helmholtz equation. The latter is defined as

$$G_{0\Lambda}(\sigma, \mathbf{k}, \mathbf{R}) = \sum_{\mathbf{r}_s \in \Lambda} G_0(\sigma, \mathbf{R} - \mathbf{r}_s) e^{i\mathbf{k} \cdot \mathbf{r}_s} = \sum_{\mathbf{r}_s \in \Lambda} G_0(\sigma, \mathbf{R} + \mathbf{r}_s) e^{-i\mathbf{k} \cdot \mathbf{r}_s}, \quad (3)$$

$$G_0(\sigma, \mathbf{R}) = G_0(\sigma, \mathbf{r}, \mathbf{r}') = -\frac{\exp(i\sigma R)}{4\pi R}, \quad (4)$$

where $\mathbf{R} = \mathbf{r} - \mathbf{r}'$ and $R = |\mathbf{R}|$, denotes a free-space scattering Green's function of the 3D scalar Helmholtz equation at the points \mathbf{r} and \mathbf{r}' . Within the Korringa-Kohn-Rostocker (KKR) method,¹¹ band structure is determined by solving the KKR secular equation

$$\det [1 - t(\sigma)g(\sigma, \mathbf{k})] = 0, \quad (5)$$

where t is a single-scatterer scattering T-matrix and g is the matrix of structure constants.¹¹ Both t and g in Eq. (5) are considered as matrices with matrix elements labeled by pairs of angular momentum numbers $(lm, l'm')$, where $-l \leq m \leq l$. In the scalar case, for instance, in the case of multiple-scattering scattering of electrons, the matrix elements of g in the angular-momentum basis are defined as expansion coefficients of

$$G_{0\Lambda}(\sigma, \mathbf{k}, \mathbf{R}) - G_0(\sigma, \mathbf{R}) = \sum_{lm, l'm'} g_{lm, l'm'}(\sigma, \mathbf{k}) j_l(\sigma r) Y_{lm}(\mathbf{r}) j_{l'}(\sigma r') Y_{l'm'}^*(\mathbf{r}'), \quad (6)$$

where j_l are the regular spherical Bessel functions,¹² and Y_{lm} are the conventional spherical harmonics.¹²

It is interesting to note that, to a large extent, the scalar case also covers the scattering of vector and tensorial waves, i.e., waves with a non zero spin, provided each field component independently obeys the scalar Helmholtz equation (2).^{13,14} In the vector case of multiple-scattering of electromagnetic waves, $\sigma = \omega\epsilon_h/c$, where ω is the angular frequency, c is the speed of light in vacuum, and ϵ_h is the dielectric constant of the host dielectric medium. Let $L = (lm)$ stand for a multiindex of angular momentum numbers and let A label independent polarizations. The corresponding vector structure constants $G_{AL,A'L'}$ are obtained from the scalar structure constants $g_{L,L'}$ as

$$G_{AL,A'L'} = \sum_{p,p'=-1}^1 \sum_{\alpha,\alpha'=-1}^1 U_A(l, m, p, \alpha) g_{l+p, m+\alpha; l'+p', m'+\alpha'} U_{A'}(l', m', p', \alpha'), \quad (7)$$

where the U_A 's are group-theoretical coefficients, in the current case determined by the vector-coupling Clebsch-Gordon coefficients.^{13,14} Therefore, in a numerical implementation, it is only required to make the following two modifications in the scalar KKR numerical code: (i) to include a single routine which performs the transformation of the scalar structure constants into vectorial structure constants^{9,14,16,17} and (ii) to use the routine which calculates t the single-scatterer scattering T-matrix appropriate to a given boundary value problem. The same is also true if one wants to adapt the scalar 3D KKR numerical codes which deals with clusters of more than 1000 particles of arbitrary shape and clusters of more than 1000 arbitrary impurities in a crystal.^{18,19} There seem to be no obstacle to have the photonic KKR methods^{9,13,14,16,17} dealing with clusters of more than 300 particles. The KKR method can be used for scatterers of arbitrary shape¹⁹ and is optimized for lattices of spheres.

If Λ is not a simple (Bravais) periodic lattice, i.e., there is more than one scatterer in the primitive lattice cell, the matrices t and g in Eq. (5) become matrices with entries labeled by multiindices $AL\alpha$, where A and L are as before and α runs over all the scatterers in the primitive lattice cell.¹⁵

3. PHOTONIC CRYSTALS WITH SMALL METAL INCLUSIONS

On purely experimental grounds, only the case of spheres with a metal core is investigated here. Usually, a metal shell around a dielectric core is formed by an aggregation of small metallic nanoparticles. The shell has to be around 20 nm thick before it becomes complete.²⁰ With an emphasis on photonic structures in the near infrared and in the visible, the 20 nm shell thickness then would mean a rather high threshold value of the metal filling fraction f_m (of the order of 5%). On the other hand, it is much easier to tune the metal filling fraction f_m from zero to a few percent by coating small metal nanoparticles with a dielectric in a controlled way.²¹ Moreover, a dielectric shell is necessary to prevent aggregation of the metallic particles by reducing the Van der Waals forces between them. In the latter case, a coating of roughly 20 nm is required.

The KKR method is best suited to deal with highly dispersive scatterers. Computational time with and without the dielectric constant dispersion is the same and only depends on the angular momentum cut-off parameter l_{max} in Eq. (5). As in previous work,^{16,24} only the real part of the material dielectric constant is used when the photonic band structure is calculated. It has been known that the imaginary part of a low absorbing metal has only little influence on the band structure.²² However it will be necessary to use both the real and imaginary part of the material dielectric constant when reflectance, transmittance, and absorptance are calculated. The dielectric constant of material is used as in Ref.²³

3.1. Band structure

Given a metal volume fraction f_m , the strongest effect on CPBG was found for a diamond structure. The actual metal volume fraction f_m needed to open a CPBG of more than 5% depends on the available material dielectric constant ϵ and can be kept below 1% for $\epsilon_s = 4$ (Fig. 2). Surprisingly, the inclusions have the biggest effect for the dielectric constant $\epsilon \in [2, 12]$, which is a typical dielectric constant at near-infrared and in the visible for many semiconductors and polymers. To reach convergence within 1%, the photonic band gap structure was calculated with the value of the angular-momentum cut-off $l_{max} = 8$.

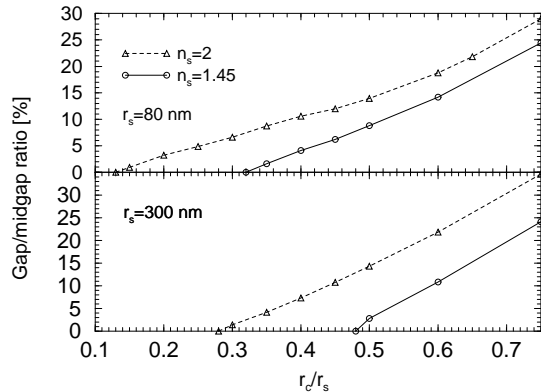


Figure 2. Calculated gap width to midgap frequency ratio of the 2nd-3rd CPBG for a close-packed diamond lattice of dielectric $n_s = 1.45$ (silica) and $n_s = 2$ (ZnS) coated silver spheres in air. The upper graph is for the sphere radius $r_s = 80$ nm and the lower graph is for the sphere radius $r_s = 300$ nm. The gap to midgap ratio is plotted as a function of the metal core radial filling fraction r_c/r_s . Metal volume fraction is then $f_m = 0.34 \times (r_c/r_s)^3$.

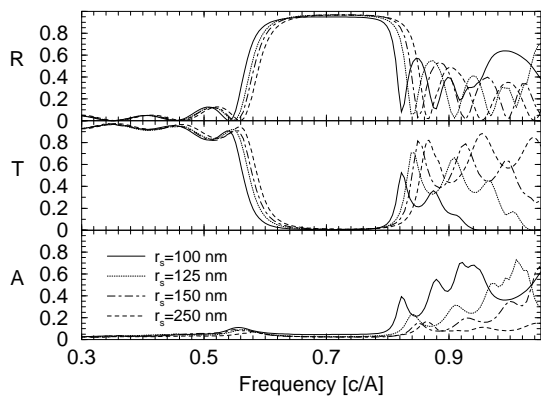


Figure 3. Reflectance, transmittance and absorptance of light incident normally on a two unit cells (12 planes) thick zinc blende lattice of spheres in air stacked in the (111) direction. One of the two spheres in the lattice primitive cell is $n_s = 1.45$ (silica) shell sphere with a silver core with fixed $r_c/r_s = 0.75$, whereas the other is a homogeneous $n_s = 1.45$ sphere of the same radius ($f_m = 7.2\%$). Dimensionless frequency is used on the x -axis, where A is the lattice constant of a conventional unit cell of the cubic lattice. In all cases, the 2nd-3rd CPBG lies between ≈ 0.7 and 0.8 and stays above 5%.

3.2. Reflection, transmission, absorption

In Fig. 3 reflectance, transmittance and absorptance of light incident normally on a two unit cells (12 planes) thick zinc blende lattice of spheres in air stacked in the (111) direction is shown. They were calculated by adapting available computer code,²⁵ which is based on the layer photonic KKR method.¹³ The same method was also used in Ref..²⁴ To reach convergence within 1% around the 2nd-3rd CPBG, $l_{max} = 6$ was used. Calculations showed that absorption can be kept at very small levels. Given the desired gap width of 5%, the smallest absorption was found for close-packed zinc-blende structures, even though the required f_m was typically twice as large as that of the close-packed diamond structure. This result suggest that, given the metal filling fraction f_m , absorption is reduced due to a reduction of near-field electromagnetic energy transfer between the metal cores with an increased separation of the metal islands in the structure. For a zinc-blende structure, absorptance within a CPBG of 5% for $\lambda \geq 750$ nm can be kept below 2.6%. The results on the absorption are by far the best which have been demonstrated for a 3D metallo-dielectric structure with a CPBG. They are

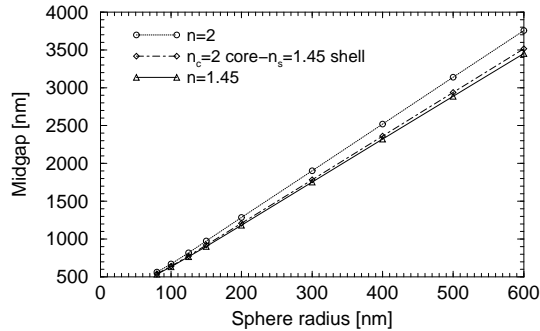


Figure 4. An example of scaling of the midgap wavelength of the 2nd-3rd CPBG for a close-packed zinc-blende lattice of spheres in air with the sphere radius. One of the two spheres in the lattice primitive cell is $n_s = 1.45$ (silica) shell sphere with a silver core with fixed $r_c/r_s = 0.75$, whereas the other is purely dielectric sphere of the same radius ($f_m = 7.2\%$). The latter is either a homogeneous $n = 1.45$ (silica) sphere, a homogeneous $n = 2$ (ZnS) sphere, or, $n_c = 2$ (ZnS) core- $n_s = 1.45$ (silica) shell sphere with fixed $r_c/r_s = 0.6$.

an order of magnitude better than for the case of an fcc lattice of metal coated spheres²⁴ and compare well to the best results for one-dimensional and two-dimensional metallo-dielectric photonic crystals which show absorptance $\approx 1\%$ and $\approx 3\%$, respectively, at $\lambda \approx 600$ nm.³ Photonic band structure calculations also revealed a surprising scaling-like behavior of our metallo-dielectric diamond and zinc blende structures (see Figs. 3, ??), which is only intrinsic to purely dielectric structures. The scaling-like behavior means that once a CPBG is found, the CPBG can be open for any wavelength, simply by scaling all the sizes of a structure - an extremely useful property from a practical point of view. A metal-core dielectric-shell sphere morphology seems to play an essential and non-negligible role in the effect of small metal inclusions on photonic band structure. For instance, a diamond structure of small metal nanospheres embedded in a dielectric matrix shows a much smaller CPBG and much higher absorptance for a comparable f_m than either a diamond or a zinc-blende close-packed structure of metal-core dielectric-shell spheres in air. If instead of a metal core the same volume of a metal is spread homogeneously within the spheres, no CPBG opens in the spectrum. In the latter case the sphere dielectric constant was calculated using the Garnett formula.⁹

4. CONCLUSIONS

For the example of a diamond and zinc blende structures of dielectric spheres it has been demonstrated that small inclusions of a low absorbing metal with volume fraction f_m can have a dramatic effect on a CPBG between the 2nd-3rd bands. Surprisingly, the inclusions have the biggest effect for $\varepsilon \in [2, 12]$, which is a typical dielectric constant at near-infrared and in the visible for many semiconductors and polymers. For example, in the case of silica spheres, the 2nd-3rd CPBG opens for $f_m \approx 1.1\%$ of silver and exceeds 5% for $f_m \approx 2.5\%$. Absorption in the 2nd-3rd CPBG of 5% remains very small ($\leq 2.6\%$ for $\lambda \geq 750$ nm). The structures enjoy scaling-like behavior, enabling one to scale the 2nd-3rd CPBG from microwaves down to ultraviolet wavelengths. Our results imply that just any dielectric material can be used to fabricate a photonic crystal with a sizeable and robust CPBG in three dimensions. These findings (i) open a door for many other semiconductor and polymer materials to be used as genuine photonic crystal building blocks and (ii) significantly increase the possibilities for experimentalists to realize a CPBG in the visible. Moreover, due to a high sensitivity of a CPBG on f_m , one has the freedom to engineer g_w from zero to more than 60%.

ACKNOWLEDGMENTS

I like to thank my colleagues A. van Blaaderen, A. Imhof, M. Megens, and K. P. Velikov for careful reading of the manuscript and useful comments. SARA computer facilities are also gratefully acknowledged.

REFERENCES

1. V. P. Bykov, "Spontaneous emission from a medium with a band spectrum," *Sov. J. Quant. Electron.* **4**, 861–871 (1975).
2. E. Yablonovitch, "Inhibited spontaneous emission in solid-state physics and electronics," *Phys. Rev. Lett.* **58**, 2059–2062 (1987).
3. *Photonic Crystals and Localization in the 21st Century*, Proceedings of the NATO ASI School, C. M. Soukoulis, ed., Kluwer Academic, Dordrecht, 2001.
4. K. M. Ho, C. T. Chan, and C. M. Soukoulis, "Existence of photonic gap in periodic dielectric structures," *Phys. Rev. Lett.* **65**, 3152–3155 (1990).
5. E. Yablonovitch, T. J. Gmitter, and K. M. Leung, "Photonic band structure: The face-centered-cubic case employing nonspherical atoms," *Phys. Rev. Lett.* **67**, 2295–2298 (1991).
6. A. Mekis, J. C. Chen, I. Kurland, S. Fan, P. R. Villeneuve, and J. D. Joannopoulos, "High transmission through sharp bends in photonic crystal waveguides," *Phys. Rev. Lett.* **77**, 3787–3790 (1996).
7. Z.-Y. Li and Z.-Q. Zhang, "Fragility of photonic band gaps in inverse-opal photonic crystals," *Phys. Rev. B* **62**, 1516–1519 (2000).
8. A. Moroz, "Photonic crystals at near-infrared and optical wavelengths", to appear in the Proceedings of the MRS Fall Meeting 2001.
9. A. Moroz and C. Sommers, "Photonic band gaps of three-dimensional face-centered cubic lattices," *J. Phys.: Condens. Matter* **11**, 997–1008 (1999).
10. B. G. Levi, "Visible Progress made in three dimensional photonic crystals," *Phys. Today*, 17–19, January (1999).
11. W. Kohn and N. Rostoker, "Solution of the Schrödinger equation in periodic lattices with an application to metallic lithium," *Phys. Rev.* **94**, 1111–1120 (1954).
12. *Handbook of Mathematical Functions*, M. Abramowitz and I. A. Stegun, eds., Dover Publications, 1973.
13. A. Modinos, "Scattering of electromagnetic waves by a plane of spheres-formalism," *Physica* **141**, 575–588 (1987).
14. A. Moroz, "Density-of-states calculation and multiple scattering for photons," *Phys. Rev. B* **51**, 2068–2081 (1995). See also X. Wang, X.-G. Zhang, Q. Yu, and B. N. Harmon, "Multiple-scattering theory for electromagnetic waves," *Phys. Rev. B* **47**, 4161–4167 (1993).
15. B. Segall, "Calculation of the band structure of "complex" crystals," *Phys. Rev.* **105**, 108–115 (1957).
16. A. Moroz, "Three-dimensional complete photonic-bandgap structures in the visible," *Phys. Rev. Lett.* **83**, 5274–5277 (1999).
17. A. Moroz, "Photonic crystals of coated metallic spheres," *Europhys. Lett.* **50**, 466–472 (2000).
18. J. S. Faulkner, "Scattering theory and cluster calculations," *J. Phys. C: Solid State* **10**, 4661–4670 (1977).
19. W. H. Butler, A. Gonis, and X.-G. Zhang, "Multiple-scattering theory for space-filling cell potentials," *Phys. Rev. B* **45**, 11527–11541 (1992).
20. C. Graf and A. van Blaaderen, "Metallodielectric Colloidal Core-Shell Particles for Photonic Applications," *Langmuir* **18**, 524–534 (2002).
21. L. M. Liz-Marzán, M. Giersig, and P. Mulvaney, "Synthesis of nanosized gold-silica core-shell particles," *Langmuir* **12**, 4329–4335 (1996).
22. V. Kuzniak and A. A. Maradudin, "Photonic band structures of one- and two-dimensional periodic systems with metallic components in the presence of dissipation," *Phys. Rev. B* **55** 7427–7444 (1997).
23. *Handbook of Optical Constants of Solids*, E. D. Palik, ed., Academic, New York, 1985.
24. Z. Wang, C. T. Chan, W. Zhang, N. Ming, and P. Sheng, "Three-dimensional self-assembly of metal nanoparticles: Possible photonic crystal with a complete gap below the plasma frequency," *Phys. Rev. B* **64**, 113108 (2001).
25. V. Yannopoulos, N. Stefanou, and A. Modinos, "Heterostructures of photonic crystals: frequency bands and transmission coefficients," *Comp. Phys. Commun.* **113**, 49–77 (1998).